New trends in non–destructive assessment of aerospace structures

Wieslaw M. Ostachowicz*[a,b], Pawel H. Malinowski[a], Tomasz Wandowski[a],
[a]Polish Academy of Sciences, Institute of Fluid–Flow Machinery
14 Fiszera Street, 80–231, Gdansk, Poland;
[b]Warsaw University of Technology, Faculty of Automotive and Construction Machinery
84 Narbutta Street, 02–524 Warsaw, Poland

ABSTRACT

The scope of the paper includes non–destructive assessment of the structure's material condition, for the aerospace structures during its useful lifetime. The paper presents multidisciplinary technologies devoted to development and implementation of methods and systems that realize inspection and damage detection by non–destructive methods.

The paper covers several disciplines which are based on topics such as piezoelectric transducers, elastic waves propagation phenomenon, structural vibrations analysis, electro–mechanical impedance method, terahertz technique, laser induced fluorescence and 3D laser vibrometry applications.

Among various techniques available the paper presents selected numerical simulations and experimental validations of considered structures. Authors address also the problem of adhesive bonding in the case of carbon fiber reinforced polymers (CFRP). Techniques for detection of weak bonds are presented together with signal processing approaches. The reported investigations concern weak adhesive bonds caused by both manufacturing (e.g. release agent, poor curing) and in–service contaminations (e.g. moisture). Also the paper provides helpful information about dispersion, mode conversion and wave scattering from stiffeners and boundaries. It addresses the problem of optimisation of excitation signal parameters and sensor placement, as well as analysis of signals reflected from damage. It also includes a variety of techniques being related to diagnostics (damage size estimation and damage type recognition) and prognostics.

Keywords: CFRP, composites, aluminium, NDT, NDE

1. INTRODUCTION

Contemporary aerospace structures are made with various materials. Aluminum alloy, GLARE, CFRP, GFRP are widely used and the up-to-date NDT techniques should handle with the wide range of materials. Moreover, not only typical damage as cracks and delamination [1], [2] should be considered but also it is important to assess the surface quality and the structural bonds performance. The adhesive bonding is present at the manufacturing process as well as in service in the form of composite repair patches used for repairs. Previous research proved that fluid absorption influences the mechanical performance of composites [3],[4] so the a NDT for detecting the presence of a fluid would be crucial for ensuring the integrity of the structure. The performance of adhesive bonds depends on the physico-chemical properties of the adhered surfaces. In [5] the effect of pre-bond release agent and moisture absorption on mode-I fracture toughness of CFRP bonded joints was qualitatively and quantitatively studied. It was shown that the release agent contamination may lead to about 60% drop of critical crack energy release rate (GIC). Improperly chosen curing temperature of the adhesive leads also to changes even up 95% reduction of GIC for temperature lower by one third [6]. This indicates that the effective NDT methods should have a broad spectrum of usage and it is not to be expected that only one methods would be suitable for all these tasks, therefore new techniques are sought and investigated.

This paper is divided into three major sections. Firstly, the methods and examples for surface assessment are presented. Secondly, the methods and real experimental examples for structural joints assessment are described. In the last part the methods and results for damage detection and localization are gathers. The paper ends with concluding section.

Sensors and Smart Structures Technologies for Civil, Mechanical, and Aerospace Systems 2015,
edited by Jerome P. Lynch, Kon-Well Wang, Hoon Sohn, Proc. of SPIE Vol. 9435, 943502
 · doi: 10.1117/12.2178155

2. NDT METHODS FOR SURFACE ASSESSMENT

In this section three NDT methods were presented with focus on surface assessment. The presented results are based on CFRP samples analysis. The first investigated method is the Electromechanical impedance (EMI). The EMI method is considered as one of the NDT or SHM methods. It uses a piezoelectric sensor that is bonded to the inspected host structure. During the measurement basic electric parameters of the sensor are gathered. Parameters such as resistance, reactance, impedance, conductance, etc. are measured and analyzed. These quantities are measured as a function of frequency. Due to direct and converse piezoelectric effect the sensor excites and senses the response from the host structure. This electromechanical coupling causes that the registered impedance spectra are modified by the presence of the host structure. Moreover if there is a damage or some other discontinuity this has also its influence on the registered spectra. Appearance of additional resonance peaks, peak shift in frequency or magnitude change can be treated as indicator of defect of the host structure [7]. One also should not forget that the sensors for EMI technique is bonded to the structure and the bonding itself has an influence on the response [8],[9].

Using the EMI method the influence of moisture absorbed by CFRP was investigated. The sample was a three layer prepreg. Five chosen stages of absorption process were considered. In first case electrical impedance was registered for a dry sample. In the second case the electrical impedance was measured after thirteen days of sample immersion in water. In the third case the same measurements were performed for sample after one day of drying in the room temperature. In the case number four measurements were repeated after two days of sample drying in the room temperature. Finally, in the case number five measurements were repeated after five days drying also in the room temperature.

The moisture influence was observed in the real part of electrical impedance (resistance) in range 0-550 kHz (Figure 1). The increasing moisture level caused shifts of the peaks to the left. Peaks in the real part of the electromechanical impedance are directly related to natural frequencies of CFRP sample [10], [11]. This fact can be related to the reduction of natural frequencies values. Due to moisture uptake sample mass increases what results in reduction of natural frequency values. On the other hand moisture content allow to reduce stiffness what also reduces natural frequency values [12]. Moisture content causes degradation of elastic modulus.

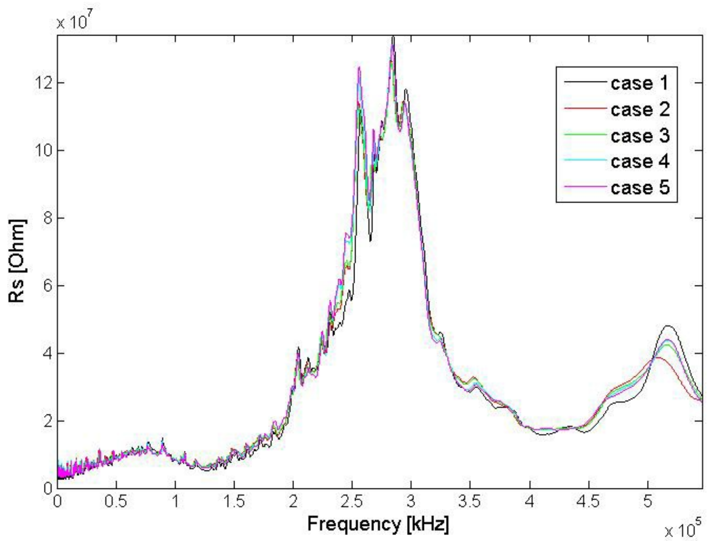

Figure 1. Real part of electrical impedance spectra of piezoelectric transducer for moisturized sample.

In order to characterize the changes of real part of the electromechanical impedance due to moisture level a deviation index (DI) was utilized [10]. The first case (dry sample) was taken as referential state and next four cases were taken as unknown states (Figure 2). Deviation index values calculated for whole investigated frequency band presented in figure 1.

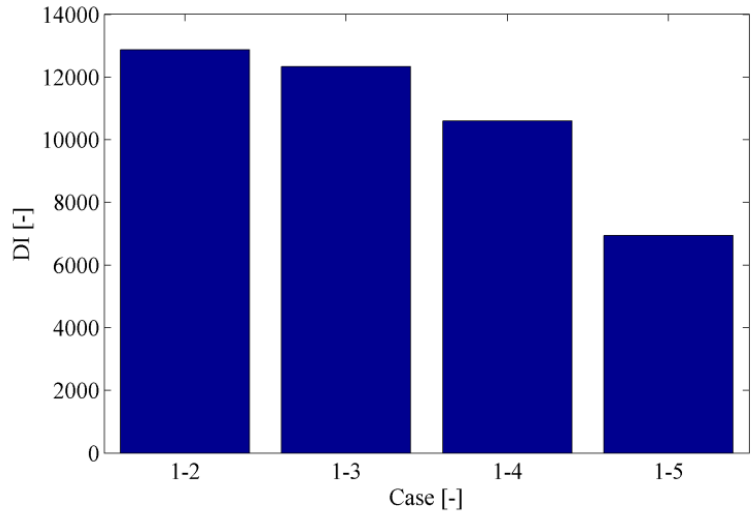

Figure 2. Deviation index values for investigated cases.

Largest value of DI was obtained for case 1-2. In this case DI was calculated based on signal for referential state measurements (dry sample) and state of sample taken out of the water after thirteen days. In this case moisture level is highest. Smaller value of DI can be observed for case 1-3 based on measurements taken after one day of drying. Value of DI decrease further for case 1-4 which is related to the measurements after two days of sample drying. The smallest DI value was achieved in the case 1-5 related to the measurements after five days drying.

Analyzing the frequency shifts in the vicinity of 285 kHz (Figure 1) it can be noticed that plot of spectra for the case number two (after thirteen days moisture uptake) is shifted to the left (by 1700 Hz) in comparison to the spectra for sample from case one (dry condition – reference state). In the third case (after one day drying) compared to second case characteristic shift a little bit back to the right (by 200 Hz). After second day of sample drying (fourth case) resistance characteristic is shifted more and also to the right (by 600 Hz). Next for measurements after seven day long drying process measured characteristic is shifted most to the right (by 200 Hz). Finally in the last case frequency of observed peak is placed 700 Hz to the left in relation to the referential state.

Based on these result one can concluded that for increasing level of moisture characteristic of real part of transducer electrical impedance is shifting to the left. For decreasing moisture level characteristic is shifted back to the right. Increasing level of moisture causes reduction of maximum peak amplitude. For decreasing level of moisture amplitude of maximum peak increase almost to the value for referential state. Region around frequency 285 kHz was taken into considerations due to fact that resonance peaks have maximum amplitude in this region. According to [10] frequency band with highest density of peaks is recommended for the analysis.

The second investigated method for surface assessment was base on Laser Doppler Vibrometry (LDV) used for guided wave sensing. Vibrometry measurements were conducted with scanning laser vibrometer working in 1D mode (V in figure 3). During the measurement the sample surface (S in figure 3) is scanned by a red laser beam. The samples were excited with a piezoelectric transducer (T in figure 1). The transducer was a disc with diameter: 10 mm and thickness: 0.5 mm (CeramTec, material: SONOX P502). The excitation signal was a tone burst with 5 cycles. The used vibrometer is a scanning device that allowed to measure response at various points at the surface without the need for moving the sample or scanning head.

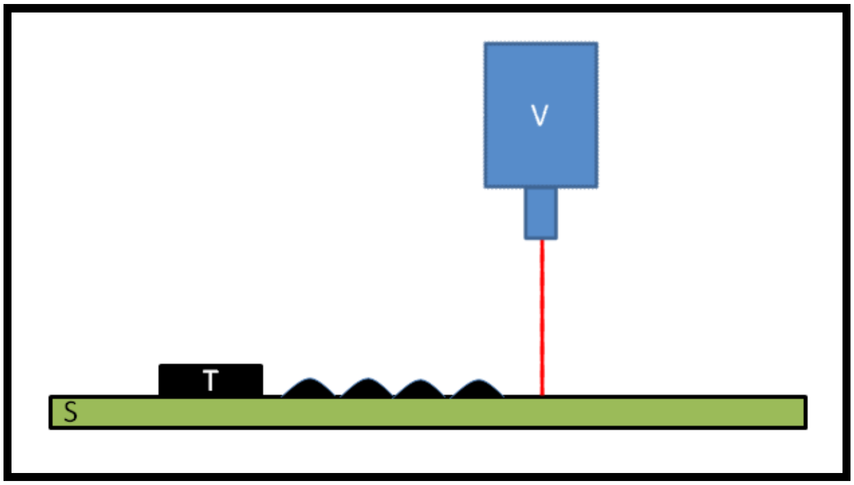

Figure 3. Measurement scheme for vibrometry method.

Research was focused on CFRP samples contaminated with moisture (MO) and hydraulic fluid (SK). Moreover thermally degraded samples (TD) were tested. The samples were prepared in the frame of FP7 ENCOMB project. The materials used in the manufacture of the basic plates were HEXCEL M21 and T700. The manufacture was performed by Airbus Nantes.
Four moisture cases were considered 0.2, 1.0, 1.1 and 1.3 % increase in weight (respective symbols: MO1-MO4). Three level of water solution of hydraulic fluid (Skydrol) was considered giving the different pH value: 4,3 and 2 (respective symbols: SK1-SK3). In the case of thermal degradation there were also three cases represented by temperature at which the samples were kept in air circulated oven: 190, 200 and 210 ^{o}C (respective symbols: TD1-TD3). The reference sample (uncontaminated, untreated thermally) was marked as Ref.
In order to perform surface assessment following signal processing was proposed. At each measurement point an index proportional to squared signal was calculated. This index is proportional to squared voltage and can be associated with out of plane vibration energy. The calculated index was averaged over the whole set of measurement points. The sensitivity to surface anomalies were sought in the value of this energy (*E)* and its dispersion over the surface represented by standard deviation (σ). Figure 4 shows that some of the contaminated samples clearly differ from the reference. The method clearly indicates the moisture contaminated CFRP samples (MO) – left bottom corner in figure 4. Both chosen parameters (E and σ) show a significant decrease in comparison to reference (Ref). The CFRP samples contaminated by hydraulic oil (SK) characterize by slightly smaller E and σ than the reference sample. The thermally degraded samples (TD) did not differ too much from the reference.

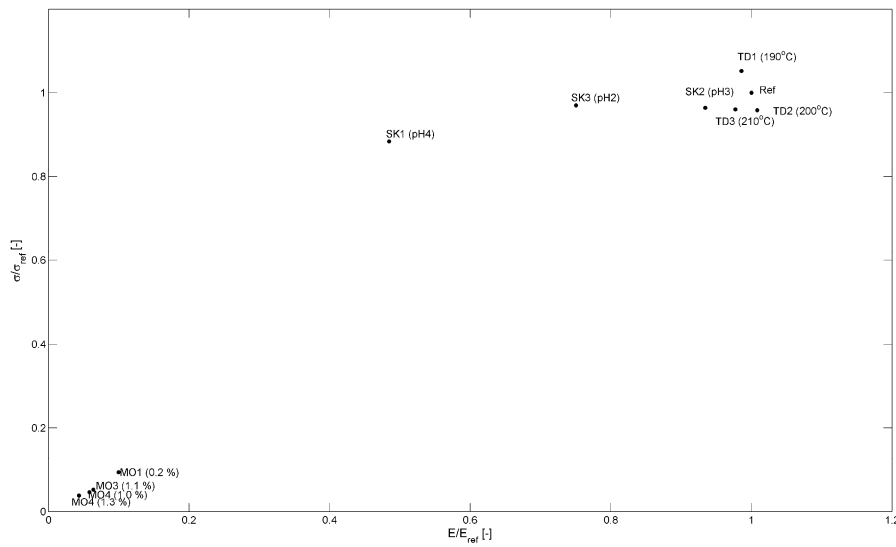

Figure 4. Results for surface characterization using laser vibrometry.

The third investigated method was fully noncontact. In this method Laser Induced Fluorescence Spectroscopy (LIF) was used. The LIF allow to analyze large objects using surface scanning technique with noncontact excitation and sensing [13] (Figure 5). The excitation source (L) is - Nd:YAG, 6 ns pulse, 1064 nm laser equipped with harmonic generation modules: 532 nm, 355 nm and 266 nm. Monochromator is used for the detection of fluorescence (D). The fluorescence spectra are recorded and processed. LIF was used for surface assessment of CFRP specimens. The LIF spectra were recorded for laser excitation at 266 nm, 355 nm and 532 nm. Applied laser intensity for all wavelengths was about 300 J/m2. The preliminary studies of the fluorescence shows that applied laser radiation does not cause degradation of investigated material and changes of fluorescence spectra in subsequent measurements. The conducted comparison of the possible excitation showed that for 266 and 355 nm there are no differences in fluorescence spectra between clean reference sample and samples contaminated with hydraulic fluid and release agent. Thermal degradation of the sample also do not caused any visible change. Under excitation at 532 nm, beside narrow band with a maximum at 432 nm (observed also for other excitation – at 266 and 355 nm), a strong fluorescence in a wide band with maximum at 600 nm is observed. The intensity of the wide band fluorescence changes significantly for different samples. The quantitative assessment of the sample surface was based on three parameters – intensity (A), fluorescence lifetime (T) and decay time (t). Fluorescence life time (T) is equal to two standard deviations after fitting a Gaussian distribution to the measured curve. Fluorescence decay time (t) is equal to amplitude drop by e and it is obtained by fitting an exponential curve to the falling slope of the measured curve. The results for SK samples show that the fluorescence lifetime (T) indicates dropping value of T with decreasing pH value. The same behavior can be observed for the decay time (t) [13]. The fluorescence intensity seems to be insensitive to hydraulic fluid contamination. Taking into consideration the TD samples it was observed that with increasing temperature of degradation the fluorescence intensity increases [13]. Due to availability of two samples for 200 and 210^0C the reliability of the method was tested. The samples of the same type gave similar result. The increasing intensity in relation to 190^0C and reference samples was observed. It should be mentioned that fluorescence lifetime and decay did not allow detect the thermal degradation. Measurements of samples contaminated with release agent solution indicated no sensitivity of the method for release agent contamination level.

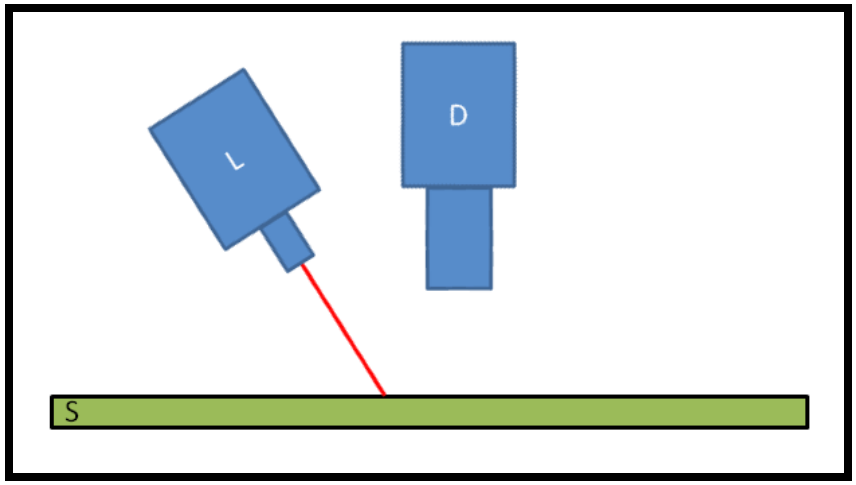

Figure 5. Measurement principle of the LIF method.

3. NDT METHODS FOR STRUCTURAL JOINTS ASSESSMENT

In this section we focus on the NDT of structural bonds. Attention was focused on performance of riveted joints and adhesive bonds of composites. The EMI technique was used for investigation of a aircraft wing section cut off from its trailing edge. The structure was composed of thin and curved upper shell which was originally fixed to the wing ribs and spars by rivets (Figure 6). For the purpose of the experiment one line of rivets was replaced by bolts in order to simulate normal and degenerate behavior of rivets in repetitive manner.

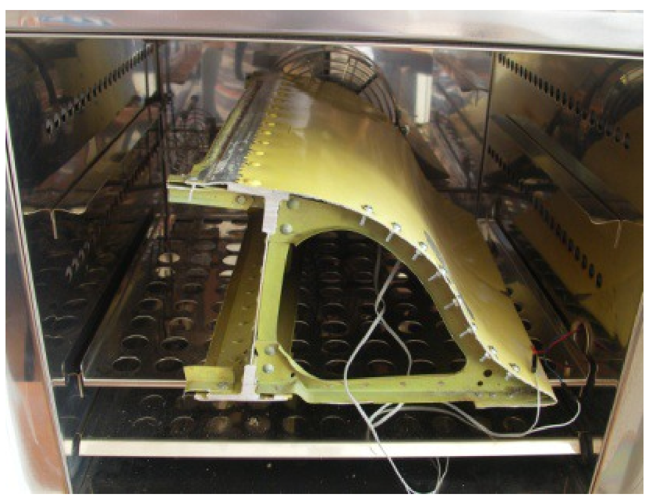

Figure 6. Section of aircraft wing in temperature chamber.

In figure 7 the sensitivity of RMSD to increased level of damage is shown for low (1-10 kHz), high (10-20 kHz) and entire (1-20 kHz) frequency intervals. Damage was introduced by subsequent loosening of three bolts connecting outer shell and internal rib in the section of aircraft wing. For stable temperature level RMSD behaves well regardless the considered frequency interval used for calculation of this damage indicator.

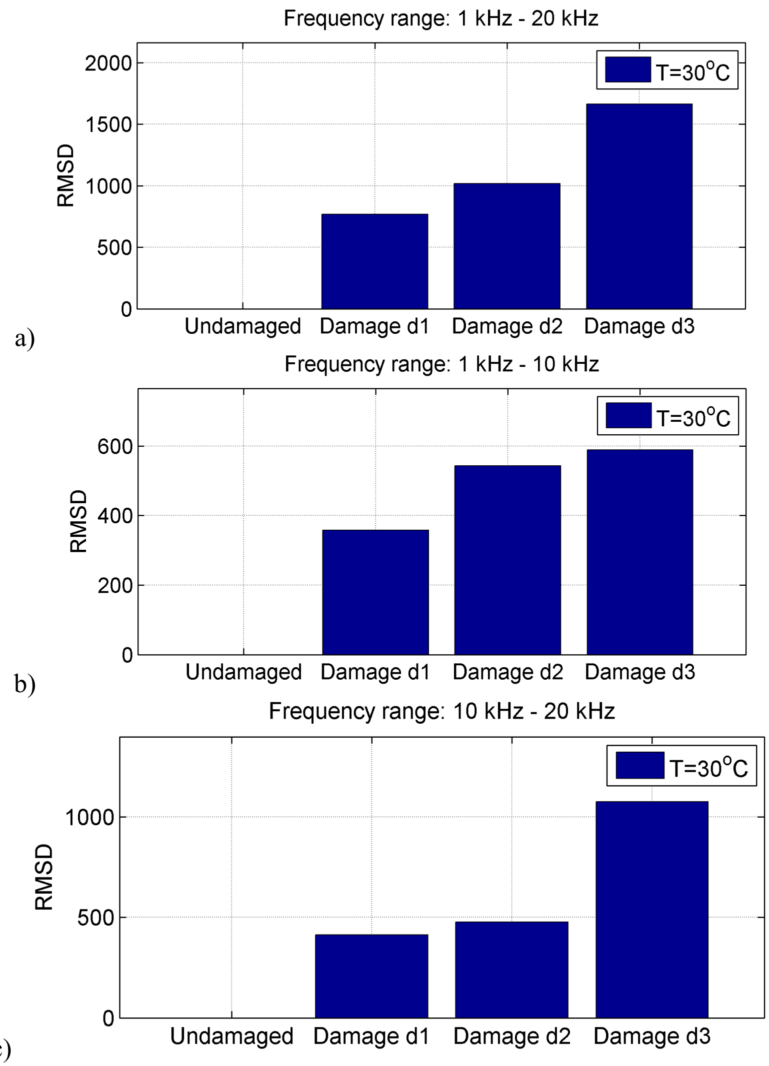

Figure 7. Performance of RMSD as damage indicator for increasing damage – measurements on the section of the wing.

The RMSD based indication gets worse if one considers indication of damage based on two measurements performed at different temperatures. If the reference measurement was performed at 30°C and the damage state measurements at 40°C, The first two cases of damage scenario were obscured by temperature differences. Only the third case d3 had bigger influence on RMSD than temperature variations [14].

The EMI methods was also used for assessment of adhesive bonds of CFRP panels. The samples were prepared in the frame of FP7 ENCOMB project. The materials used in the manufacture of the basic plates were HEXCEL M21 and T700. The manufacture was performed by Airbus Nantes. The samples for investigation were cut out of the larger basic plates. The investigated bonded samples comprised of two CFRP plates. First single plate thickness was 1.5 mm (6 plies) and it was contaminated and bonded to second sample with thickness 2.6 mm (10 plies). These samples were bonded with an adhesive film. Three different scenarios were selected for the investigation: prebond Release agent contamination (sample size 100 mm x 100 mm), prebond moisture contamination (sample size 100 mm x 50 mm) and poor curing of the adhesive (sample size 100 mm x 100 mm), The level of contamination with release agent was expressed by silicon content caused by dip coating in silicon-based release agent. The moisture uptake was described by relative mass gain. The curing temperature was an indicator for discrimination of the samples with poor curing of the adhesive. In [5] the effect of pre-bond release agent and moisture absorption on mode-I fracture toughness of CFRP bonded joints was qualitatively and quantitatively studied. A mode-I double cantilever beam (DCB) specimen was used to determine the mode-I energy release rate (GIC) referring to crack initiation. The RE1 contamination does not seem to affect the bond strength. The results for the RE2 show almost 60 % drop in GIC in comparison to REF samples. The RE3 and RE4 are characterized by very low GIC values indicating a very weak bond. The average crack initiation values of GIC for moisture samples indicate slightly different behaviour. MO1 is characterized by higher average GIC value. In case of MO2, MO3 and MO4 there is a decrease in GIC values in relation to REF. However these three categories are not easily distinguishable due to the high standard deviation of the results. In the case of CS the lower temperature of curing is expected to have great impact on bond performance. The GIC for sample cured at 120 ^{0}C drops nearly by 95% in relation to GIC for properly cured sample [5].

In the frame of this work we investigated 4 samples contaminated with moisture (MO1-0.45% MO2-0.8%, MO3-1.13%, MO4-1.25% weight increase). There were 4 samples contaminated with release agent(RE1-2.1at.%, RE2-6.5at.%, RE3-8.2at.%, RE4-10.1at.% of silicon). In the case of last scenario, poor curing, there were three samples measured (CS1-170 ^{o}C, CS2-160 ^{o}C, CS3-150 ^{o}C, curing temperature).

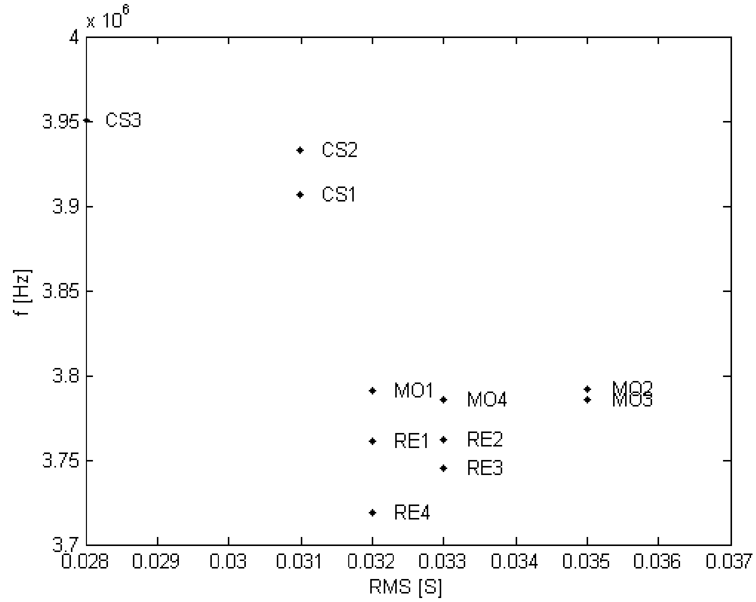

Figure 8. Peak frequency and RMS for the weak bond samples compared with results for sensors and bonded sensors.

The results of calcualtion of conductance maximum freqency *f* and *RMS* in band 3-5 MHz are depicted in figure 5. One can notice that RMS value does not allow for clear clasification of different bonding scenario. Looking at the frequencies we do not observe such separation. Only the CS1-3 and MO4* samples were clearly separated. The freqency values allow to separate some of the results. There is also indication of weak bond condition. This is better visible in figure 6, where one can notice that the decrease in the curing temepratture cases the clear increse in f (CS samples). In the case of release agent samples (RE) the weaker the bond (increse in in contamination) the lower the freqency. Moisture samples (MO) are comaprable with each other in terms of frequency.

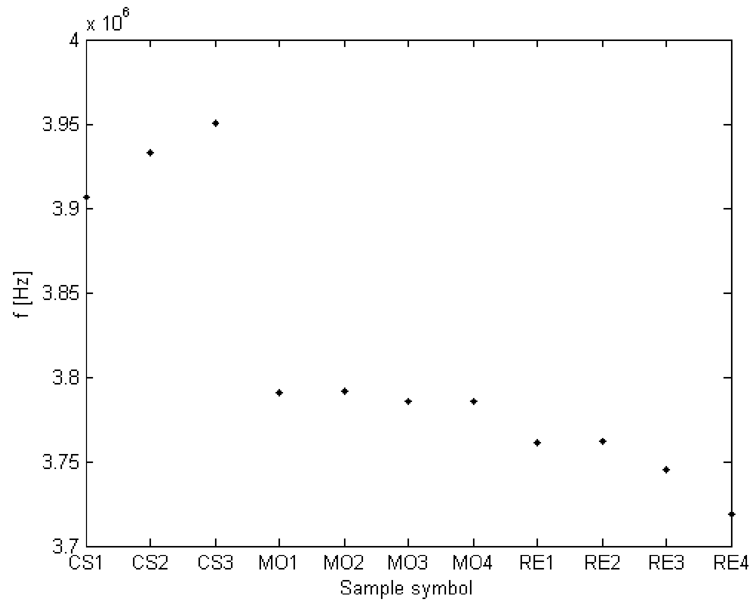

Figure 9. Weak bond influence on the frequency of the conductance peak.

The adhesive bonding was also assessed using LDV for measuring guided wave propagation (Figure 3). The LDV methodology was described in previous section related to surface assessment. The sensitivity to weak bond was sought in the value of energy (*E)* and its dispersion over the surface represented by standard deviation (σ). Figure 10 shows that moisture contaminated samples (MO) clearly differ from the reference. Both chosen parameters (*E* and σ) show a significant increase in comparison to reference (Ref). The poorly cured samples (CS) also differ from the reference (Figure 11). Moreover the lower the curing temperature the difference is growing. In the case of release agent contaminated (RE) samples (not shown in figure) a significant difference was not observed.

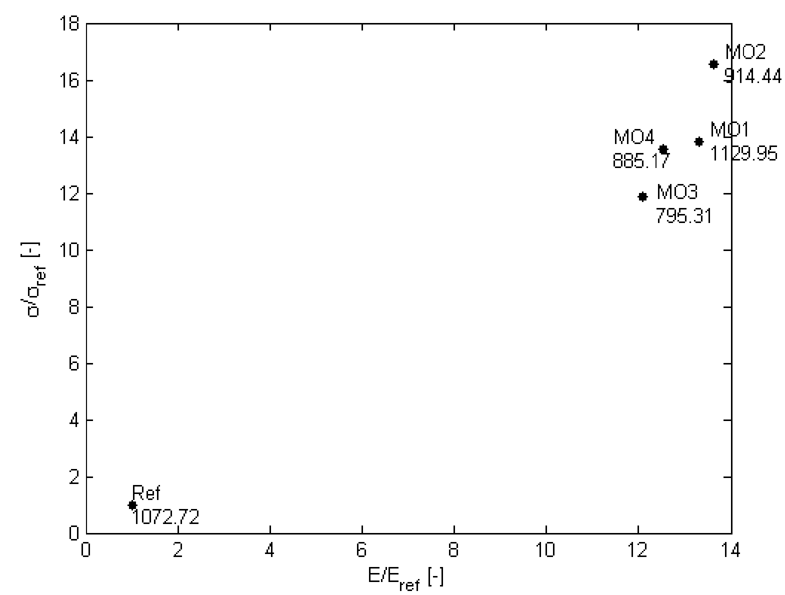

Figure 10. Results for moisture contaminated bonds characterization using laser vibrometer; next to the sample symbol the mean GIC value was provided.

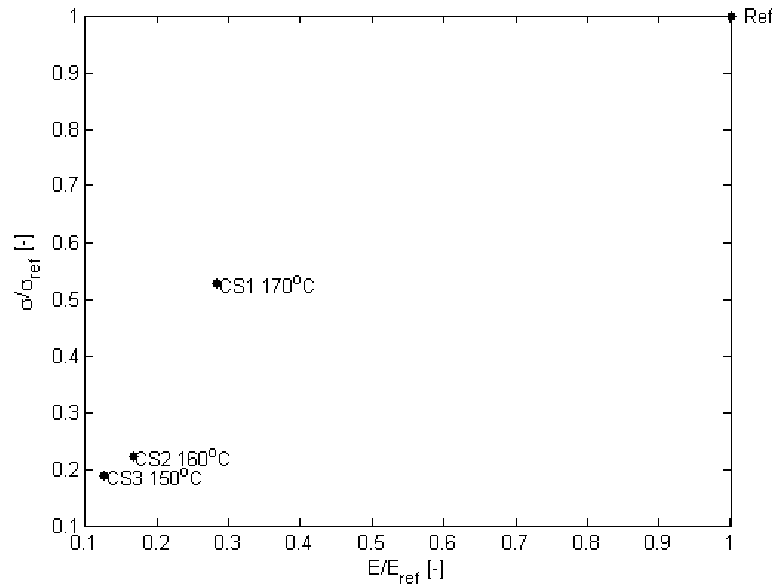

Figure 11. Results for poorly cured bonds characterization using laser vibrometer; next to the sample symbol the curing temperature was provided.

4. NDT METHODS FOR DAMAGE DETECTION

In this section authors focus on methods aimed at damage detection. The first investigated method is the terahertz time-domain spectroscopy (TDS) [15]. This is a spectroscopy in the frequency range from 100 GHz to around 4 THz that has been used in recent years for the purpose of non-destructive material testing. The submillimeter-waves are able to penetrate through many nonconducting materials. At each dielectric interface, e.g. from air to the GFRP material, the electromagnetic waves experience partial transmission and reflection. In this paper, we use the THz-TDS-system as a tool to remotely detect delamination presence. The scanning heads of the THz-TDS-system worked in reflection mode. THz TDS system TPS Spectra 3000+ by TeraView Limited generates radiation in the form of repeated, very narrow picosecond pulses which are focused and sent toward the investigated structure. Wide frequency content, small power and non-ionizing radiation are the main characteristics of the pulse. This approach is very interesting when the material allow for penetration at THz-frequencies, such as GFRP. The experimental setup using THz TDS system is shown in Figure 12. The investigated samples are supported by steel bars mounted to system responsible for the movement in the horizontal plane.

Figure 12. Therhertz TDS spectrometer with scanning unit

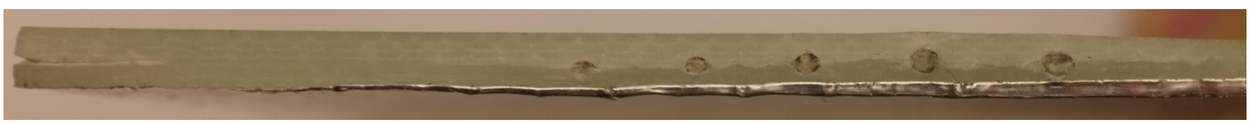

Figure 13. GFRP sample with artificially introduced delamination

The investigated sample was a GFRP with artificially introduced delamination (Figure 13). The bottom part of the sample was covered with metallic adhesive tape in order to amplify the radiation reflection that can be observed in registered signals. The whole area of the sample was scanned with fine step. The time signal registered for damage free area of the sample is depicted in figure 14. The highest pulse reflected for the upper surface is visible at about 10 ps. There are some subsequent smaller pulse representing the internal structure. The pulse reflected from sample end is visible at about 55 ps.

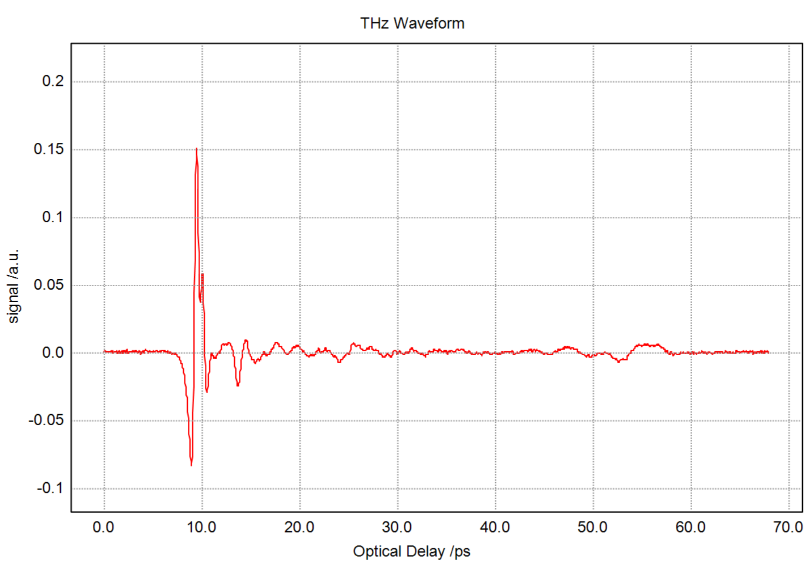

Figure 14. THz reflection signal registered at damage free area

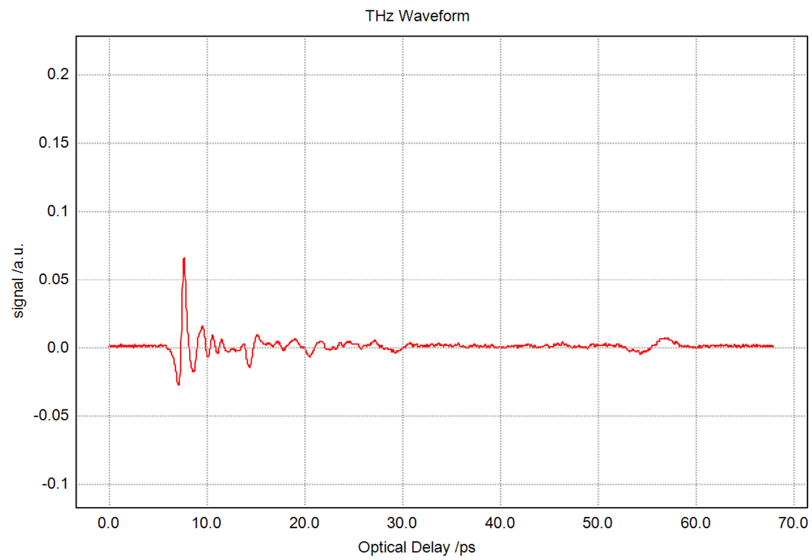

Figure 15. THz reflection signal registered at delamination area

Looking at the terahertz signal for delaminated area one can notice a weak reflection at about 28 ps (Figure 15). This is related to presence of delamination at about half of the cross section. The registered time signals are basis for B-scan and C-scan visualization that is analogous to visualization technique used in traditional ultrasonic testing.

The second efficient method for damage detection is based LDV measurements. The methodology is similar to these described in sections about surface and bond assessment. However the signal processing used here is a bit different. For damage localization purposes authors do not look at the average values for the whole surface but at local changes. For this reason we used the RMS values assigned to the locations of vibrometer measurement points [16].

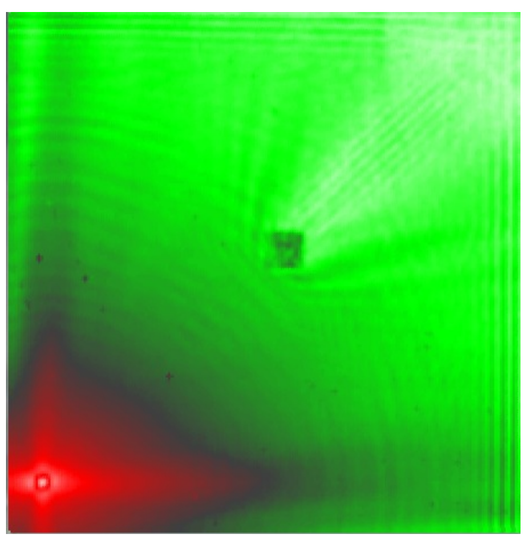

Figure 16. Visualization of delamination location for LDV registered guided waves at 100 kHz; delamination: 20 mm x 20 mm THz reflection signal registered at delamination area

The investigated case was a 500 m x 500 mm x 2 mm CFRP plate with artificial delamination in the form of a teflon insert (20 mm x 20 mm). Only one quarter of it was measured with the scanning LDV. The excitation signal was a 100 KHz tone burst with 5 cycles. The damage detection result is depicted in figure 16. In the left lower corner there is a high value of RMS representing the location of the transducer. The wave scattering at the delamination caused that the RMS values reflect the real rectangular shape of the inserted Teflon (middle part of figure 16).

The presence of structure failure can be also visualized by LDV looking at guided wave mode conversion [17]. Authors investigated a aircraft panel with riveted stiffeners. In figure 17 chosen frames from animation of elastic wave propagation in referential panel (a) and a panel with removed rivet (b) were presented. In these frames from wave propagation mode conversion (symmetric to antisymmetric S/A) caused by rivets is clearly visible. What is interesting, after removing of one rivet (location of removed rivet visible in Figure 17b – on the left part of stiffener) mode conversion was not noticed in the place without rivet (please compare figure 17a and b).

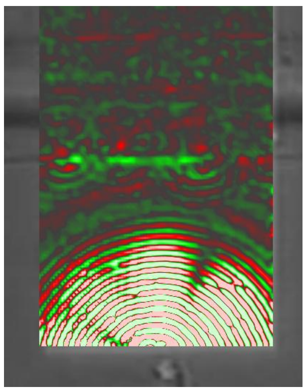

a)

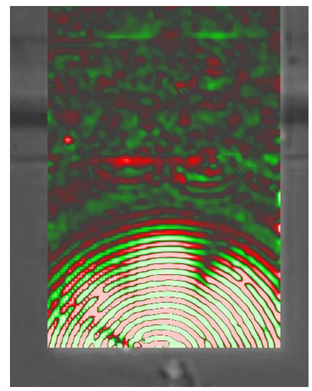

b)

Figure 17 mode conversion on rivets: a) stiffener with all rivets, b) one rivet removed; excitation frequency 200 kHz.

5. CONCLUSIONS

The effective NDT methods for aerospace applications were presented. Some of the methods (THz TDS, LIF) are totally noncontact while some need contact sensors (EMI, LDV). However the LDV could be a noncontact when it is used with laser excitation. The reported research involved metallic, CFRP and GFRP elements. The methods were successfully applied to surface assessment, joints assessment and damage detections. It was observed that some of the techniques do not provide meaningful results. The LIF method was not sensitive to release agent contamination. Due to physical limitations the THz TDS do not penetrate metallic parts and has a limited penetration depth in CFRP parts. All of the described techniques are developed further by the authors and new results will be reported in future scientific publications.

ACKNOWLEDGEMENTS

This project has received funding from the European Union's Seventh Framework Programme for research, technological development and demonstration under grant agreement no 266226.
The research leading to these results has been partially supported by project funded by Polish National Science Center under the decision no. DEC-2013/11/D/ST8/03355.
This work was partially supported by the grant no. PBS1/B6/8/2012 (project KOMPNDT) of Polish National Centre for Research and Development (NCBIR).

REFERENCES

[1] Su, Z. and Ye, L., [Identification of damage using Lamb waves], Springer-Verlag, Berlin Heidelberg, (2009).

[2] Wandowski, T., Malinowski, P., Kudela, P. and Ostachowicz, W., “Guided wave-based detection of delamination and matrix cracking in composite laminates” Proceedings of the Institution of Mechanical Engineers Part C-Journal of Mechanical Engineering Science 225, 123-131 (2011).
[3] Sala, G., “Composite degradation due to fluid absorption” Composites: Part B 31, 357-373 (2000).
[4] Pantelakis, Sp. G., Katsiropoulos, Ch. V., Tserpes, K.I. and Felgeyrolles, Th., “Effect of water absorption on strength of the aeronautical composite material Fiberdux HTA/6376” Key Engineering Materials 417-418, 457-460 (2010).
[5] Markatos, D.N., Tserpes, K.I., Rau, E. and Pantelakis, S., “Degradation of mode I fracture toughness of CFRP bonded joints due to release agent and moisture pre bond contamination” The Journal of Adhesion 90 (2), 156 – 173 (2014)
[6] Markatos, D.N., Tserpes, K.I., Rau, E., Markus, S., Ehrhart, B. and Pantelakis, Sp., “The effects of manufacturing-induced and in-service related bonding quality reduction on the mode-I fracture toughness of composite bonded joints for aeronautical use” Composites Part B: Engineering 45 (1), 556–564 (2013).
[7] Bhalla, S., Gupta, A., Bansal, S., “Ultra Low-cost Adaptations of Electro-mechanical Impedance Technique for Structural Health Monitoring” Journal of Intelligent Material Systems and Structures 20, 991-999 (2009).
[8] Moharana, S. and Bhalla, S., “Influence of adhesive bond layer on power and energy transduction efficiency of piezo-impedance transducer” Journal of Intelligent Material Systems and Structures 1045389X14523858, first published on February 25, 2014.
[9] Bhalla, S. and Moharana, S. “A refined shear lag model for adhesively bonded piezo-impedance transducers” Journal of Intelligent Material Systems and Structures 24 (1), 33-48 (2013).
[10] Giurgiutiu V., [Structural Health Monitoring with Piezoelectric Wafer Active Sensors], Elsevier, (2008).
[11] Skarbek, L, Wandowski, T, Opoka, S, Malinowski, P. and Ostachowicz, W., “Electromechanical Impedance Technique and Scanning Vibrometry for Structure Characterization” Proc. of 6th European Workshop on Structural Health Monitoring 1, 179-185 (2012).
[12] Ram Sai, KS and Sinha, PK., “Hygrothermal Effects on the Free Vibration of Laminated Composite Plates” Journal of Sound and Vibration 158 (1), 133-148 (1992).
[13] Malinowski, PH, Sawczak, M., Wandowski, T., Ostachowicz, WM and Cenian, A., “Characterisation of CFRP surface contamination by laser induced fluorescence” Health Monitoring of Structural and Biological Systems 2014, Proc. of SPIE 9064, 90640E
[14] Wandowski, T., Opoka, S., Malinowski, P. and Ostachowicz, W., “The performance of three Electromechanical Impedance damage indicators on structural element with bolted joints” Proc. of NDT in Aerospace symposium, The e-Journal of Nondestructive Testing 20 (1), (2015).
[15] Palka, N., Miedzinska, D., “Detailed non-destructive evaluation of UHMWPE composites in the terahertz range” Optical and Quantum Electronics 46 (4), 515-525 (2014).
[16] Zak, A., Radzienski, M., Krawczuk, M. and Ostachowicz, W., “Damage detection strategies based on propagation of guided elastic waves” Smart Mater. Struct. 21, 035024 (18pp), (2012).
[17] Wandowski, T., Malinowski, P. and Ostachowicz, W., “Guided waves-based damage localization in riveted aircraft panel” Health Monitoring of Structural and Biological Systems 2013, Proc. of SPIE 8695, 869519 (2013).